

## THE DENSITY PROFILE OF CLUSTER-SCALE DARK MATTER HALOS

HÅKON DAHLE, STEEN HANNESTAD

NORDITA, Blegdamsvej 17, DK-2100 Copenhagen Ø, Denmark

dahle@nordita.dk  
JESPER SOMMER-LARSEN

Theoretical Astrophysics Center, Juliane Maries Vej 30, DK-2100 Copenhagen Ø, Denmark

ApJL, in press

## ABSTRACT

We measure the average gravitational shear profile of 6 massive clusters ( $M_{\text{vir}} \sim 10^{15} M_{\odot}$ ) at  $z = 0.3$  out to a radius  $\sim 2h^{-1}$  Mpc. The measurements are fitted to a generalized NFW-like halo model  $\rho(r)$  with an arbitrary  $r \rightarrow 0$  slope  $\alpha$ . The data are well fitted by such a model with a central cusp with  $\alpha \sim 0.9 - 1.6$  (68% confidence interval). For the standard-NFW case  $\alpha = 1.0$ , we find a concentration parameter  $c_{\text{vir}}$  that is consistent with recent predictions from high-resolution CDM N-body simulations. Our data are also well fitted by an isothermal sphere model with a softened core. For this model, our  $1\sigma$  upper limit for the core radius corresponds to a limit  $\sigma_* \leq 0.1 \text{ cm}^2 \text{ g}^{-1}$  on the elastic collision cross-section in a self-interacting dark matter model.

*Subject headings:* dark matter — gravitational lensing — Galaxies: clusters

## 1. INTRODUCTION

Although the cold dark matter (CDM) model of structure formation has been successful in explaining many observable properties of the universe, there remain some notable discrepancies with observations. In particular, numerical simulations of dark matter haloes in CDM universes appear to overproduce the abundance of dark matter sub-haloes corresponding to dwarf galaxies by at least an order of magnitude (Klypin et al. 1999; Moore et al. 1999). Also, simulations indicate a transfer of angular momentum from the baryonic matter component to the non-baryonic dark matter during the assembly of disk galaxies, which leads to a conflict with the observed angular momentum properties of disk galaxies (e.g., Navarro & Steinmetz 1997, 2000; Sommer-Larsen, Götz, & Portinari 2002).

Finally, the simulations predict that dark matter halos in a wide mass range from dwarf galaxies to massive clusters follow an universal density profile with a central cusp  $\rho(r) \propto r^{-\alpha}$  with  $\alpha$  in the range  $1.0 < \alpha < 1.5$  (Navarro, Frenk, & White 1996, 1997; hereafter collectively NFW; Moore et al. 1999). This appears to be contradicted by some observations that indicate an almost constant-density core rather than a cusp, both on galaxy scales (e.g., Dalcanton & Bernstein 2000; Salucci & Burkert 2000; de Blok et al. 2001) and on cluster scales (Tyson, Kochanski, & Dell’Antonio 1998), although the interpretation of these results is controversial (e.g., Broadhurst et al. 2000; Shapiro & Iliev 2000; Czoske et al. 2002). This has led to suggestions that the dark matter properties may deviate from standard CDM, e.g., the dark matter could be warm (Colín, Avila-Reese, & Valenzuela 2000; Sommer-Larsen & Dolgov 2001), repulsive (Goodman 2000), fluid (Peebles 2000), fuzzy (Hu, Barkana, & Gruzinov 2000), decaying (Cen 2001), annihilating (Kaplinghat, Knox, & Turner 2000), self-interacting (Spergel & Steinhardt 2000; Yoshida et al. 2000, Davé et al. 2001) or both warm and self-interacting (Hannestad & Scherrer 2000). Alternatively, it has been suggested that stellar feedback from the first generation of stars formed in galaxies was so efficient that the remaining gas was expelled on a timescale comparable to, or less than, the local dynamical timescale. The dark matter subsequently adjusted to form an approximately constant density core (e.g., Gelato & Sommer-Larsen 1999). This is how-

ever unlikely to affect cluster cusps.

It is dangerous to draw wide-ranging conclusions about halo density profiles from a single object, even when based on high-quality data from strong gravitational lensing. Clearly, a larger number of clusters should be investigated using a range of methods. Other studies have sought to put constraints on  $\alpha$  from the observed abundances of strongly lensed arcs produced by clusters (Meneghetti et al. 2001; Molikawa & Hattori 2001; Oguri, Taruya, & Suto 2001), and find best fit values of  $\alpha$  similar to CDM predictions.

Previous weak lensing measurements of cluster mass profiles have usually only considered two models, a singular isothermal sphere (SIS) model with  $\rho \propto r^{-2}$  and the NFW model. Typically, it is found that the NFW model provides a marginally better fit to the data, but usually not at a very high significance (Clowe et al. 2000; Clowe & Schneider 2001; Hoekstra et al. 2002). Many of the clusters studied in this way show evidence for substructure, indicating that they may not be in dynamical equilibrium.

Here, we consider a density profile which is a generalized version of the NFW model, as described in §2. The data we present here, detailed in §3, consists of measurements of gravitational shear over a wide range of radii around 6 clusters at  $z \simeq 0.30$ . In §4 we present the results of our model fits, and in §5 we discuss the implications for cluster-scale dark matter halos and dark matter physics. We consider both a spatially-flat  $\Lambda$ CDM model with  $(\Omega_0, \lambda_0) = (0.3, 0.7)$  and a SCDM (Einstein-de Sitter) cosmology with  $(\Omega_0, \lambda_0) = (1, 0)$ , and we use  $H_0 = 100h \text{ km s}^{-1} \text{ Mpc}^{-1}$ .

## 2. HALO MODEL

Here we consider a generalized halo density profile on the form (Zhao 1996; Jing & Suto 2000)

$$\rho(r) = \frac{\delta_c \rho_c}{(r/r_s)^\alpha (1 + (r/r_s))^{3-\alpha}}, \quad (1)$$

which corresponds to the standard-NFW model for  $\alpha = 1$ , but has an arbitrary inner slope. Moore et al. (1999) favor an inner slope  $\alpha = 1.5$  and adopt a model with a slightly different functional form than we consider here, but with the same asymptotic

behavior as an  $\alpha = 1.5$  model in equation (1) for large and small scales.

NFW originally defined a concentration parameter  $c$  by  $c = r_{200}/r_s$ , where  $\bar{\rho}(r_{200}) = 200\rho_c$  and  $\rho_c$  is the critical density. For the model above, the characteristic density  $\delta_c$  is

$$\delta_c = \frac{200}{3} \left[ \int_0^1 x^2 (cx)^{-\alpha} (1+cx)^{\alpha-3} dx \right]^{-1}. \quad (2)$$

Keeton & Madau (2001) define a slightly different concentration parameter  $c_{-2} = r_{\text{vir}}/r_{-2}$ , where  $r_{\text{vir}}$  is the virial radius of the halo and  $r_{-2} = (2-\alpha)r_s$  is the radius at which  $d \ln \rho / d \ln r = -2$ . At the redshift of the clusters we examine ( $z = 0.3$ ), N-body simulations of clusters in a  $\Lambda$ CDM universe indicate that the virial radius is related to  $r_{200}$  by  $r_{\text{vir}} = 1.194r_{200} + 0.003\text{Mpc}$  (M. Götz, 2002, private communication). For the SCDM model we make the approximation  $r_{\text{vir}} \simeq r_{200}$ , since  $\bar{\rho}(r_{\text{vir}}) = 178\rho_c \simeq 200\rho_c$ .

Bullock et al. (2001) use high-resolution N-body simulations to predict the mass- and redshift-dependence of the concentration parameter  $c_{\text{vir}} = r_{\text{vir}}/r_s$  for NFW-type halos. Simulated dark matter halos show a significant dispersion about the median value of the concentration parameter at a given mass (Jing 2000), and Bullock et al. (2001) predict a scatter of  $\Delta(\log c_{\text{vir}}) = 0.18$ . Bullock et al. (2001) found the redshift-dependence of this median value to be  $c_{\text{vir}} \propto (1+z)^{-1}$ . For very massive cluster halos ( $M_{\text{vir}} \sim 10^{15}M_{\odot}$ ), the concentration is low, and  $r_s$  is of order several hundred kpc, meaning that the difference between various values of  $\alpha$  is evident even at cluster radii associated with the weak lensing regime.

### 3. LENSING DATA

The cluster sample used here was selected from a larger sample of 38 clusters targeted for weak lensing mass measurements. The data set, and the methods for data reduction and shear estimation have been described elsewhere (Dahle et al. 2002). In this letter we focus on the density profiles of a subset of six clusters of galaxies at  $z = 0.3$ . These are the most distant clusters in the sample of Dahle et al. (2002) for which wide-field imaging data exist, allowing us to probe the cluster mass profile beyond the virial radius.

The data were obtained with the UH8K mosaic CCD camera at the 2.24 m University of Hawaii telescope at Mauna Kea Observatory (see Dahle et al. 2002 for details). The clusters were selected from the X-ray luminous cluster samples of Briel & Henry (1993) and Ebeling et al. (1996), and all have X-ray luminosities  $L_{x,0.5-2.5\text{keV}} \geq 4 \times 10^{44} \text{ erg s}^{-1}$ . The virial masses  $M_{\text{vir}}$  of half of the clusters have been estimated by Irgens et al. (2002), who find values in the range  $1.1 \times 10^{15} < hM_{\text{vir}}/M_{\odot} < 3.3 \times 10^{15}$ .

The gravitational shear  $\gamma$  and convergence  $\kappa$  produced by the halo model given in equation (1) cannot be expressed in terms of simple functions, but we have derived approximate relations that are accurate to about 2% for the part of parameter space that we are able to probe with our data. The observable tangential distortion  $g_T$  is related to the tangential shear and convergence by  $g_T = \gamma_T/(1-\kappa)$  at all radii larger than the Einstein radius  $r_E$ .

As first suggested by Kaiser & Squires (1993), the signal-to-noise ratio of weak lensing observations can be boosted by ‘‘stacking’’ the weak shear measurements of a number of similar objects. Here, we stack our tangential distortion measurements for the clusters A959, A1351, A1705, A1722, A1995 and A2537, which all lie in the redshift interval  $0.285 < z < 0.325$ .

For each cluster, the average tangential distortion  $\langle g_T \rangle$  vs. radius was measured in 24 radial bins, assuming the peak in the reconstructed projected mass density (see Dahle et al. 2002) to be the cluster center.

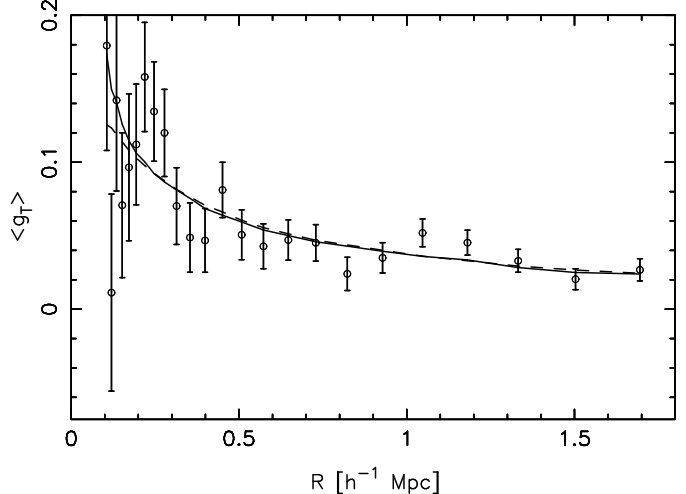


FIG. 1.— The points with error bars show the averaged gravitational lensing distortion of background galaxies as a function of radius. The solid line indicates the best fit generalized-NFW model and the dashed line indicates the best fit NSIS model. Corrections for cluster member contamination have been applied to the model curves. The physical radii plotted here are calculated for the SCDM cosmology and would be 15% larger for the  $\Lambda$ CDM cosmology.

We re-scale our clusters to the same mass (represented by a halo with velocity dispersion  $\sigma_v = 1150\text{km s}^{-1}$ , which is the average value for our clusters) using a SIS model fit to the observed tangential distortion. In doing this, we neglect the mass-dependence of the concentration parameter and the  $c_{\text{vir}} \propto (z+1)^{-1}$  redshift dependence predicted by Bullock et al. (2001). These are both only minor corrections, since the clusters we consider here have a very small spread in redshift and modest scatter in mass, and at this point we do not want to impose additional constraints on our model parameters by assuming scaling laws like those predicted by NFW or by Bullock et al. (2001). We also scale the clusters to a uniform lens redshift  $z = 0.3$  by taking into account the variation in lensing strength and angular diameter with redshift.

The faint galaxy catalogs which were used to estimate  $\langle g_T \rangle$  were generated by selecting galaxies that were detected at low significance ( $6 < \nu < 100$ ). These galaxies have typical redshifts  $z_{\text{bg}} \sim 0.9$  and typical magnitudes  $V = 24$ ,  $I = 23$ . At small projected radii from the cluster center there will be a significant fraction of cluster galaxies in the faint galaxy catalogs, and the shear estimates will be systematically biased towards lower values due to this contamination. The importance of this effect can be estimated by assuming that there is negligible contribution by cluster galaxies at the edges of the UH8K fields (i.e., beyond  $\sim 1.5h^{-1} \text{ Mpc}$ ). Thus, the true density of background galaxies can be estimated, and the cluster contribution to the faint galaxy density can be calculated in azimuthally averaged bins as a function of radius from the cluster center. By calculating the average contamination for the six clusters that go into the stack, we can significantly reduce the effects of cluster richness variations, substructure and background galaxy density fluctuations.

### 4. RESULTS

The average tangential distortion profile in a SCDM universe is shown in Figure 1 along with the best fit generalized-NFW

model curve. The 68% confidence interval for each parameter is given in Table 1 for the two cosmologies we consider. The observed profile is well represented by equation (1) for both the SCDM and  $\Lambda$ CDM case, with best fit  $\chi^2/d.o.f. = 23.66/21$  and  $22.78/21$ , respectively.

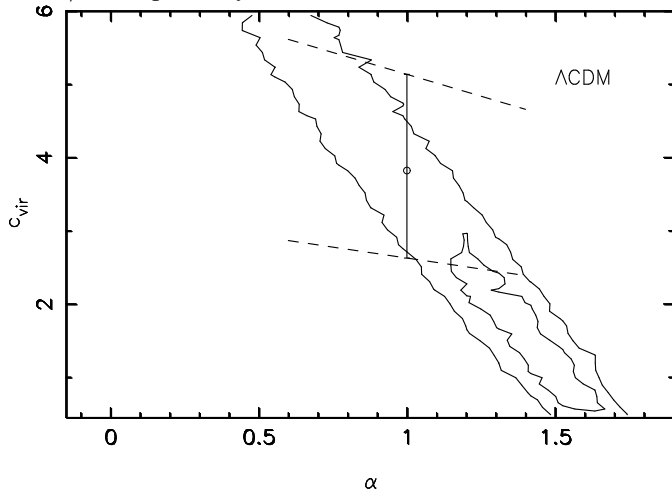


FIG. 2.— The contours indicate the 68% and 95% joint confidence intervals on  $c_{\text{vir}}$  and  $\alpha$ , derived from variations in  $\chi^2$  with respect to the minimum value. Also shown is the mean value and scatter in the concentration parameter for a  $M_{\text{vir}} = 2 \times 10^{15} M_{\odot}$  NFW halo predicted by Bullock et al. (2001) for a  $\Lambda$ CDM cosmology. The dashed lines indicate lines along which the two parameters are degenerate.

A massive central galaxy can significantly contribute to the projected mass density at small radii. Williams, Navarro & Bartelmann (1999) found that strong lensing constraints on clusters with  $\sigma_v \sim 1500 - 2000 \text{ km s}^{-1}$  are consistent with a standard-NFW profile, but  $\sigma_v \sim 1000 \text{ km s}^{-1}$  clusters are inconsistent with this model, unless the central surface density is significantly enhanced by the central galaxy. We check the robustness of our results to the inclusion of such an additional mass component by adopting a combined model which is a superposition of the dark matter profile in equation (1) and a SIS mass profile with  $\sigma_v = 300 \text{ km s}^{-1}$ . This velocity dispersion is a typical value measured for brightest cluster galaxies (e.g., Oegerle & Hoessel 1991) and is consistent with the extra central mass of  $\sim 3 \times 10^{12} h^{-1} M_{\odot}$  required to produce the arcs studied by Williams et al. (1999).

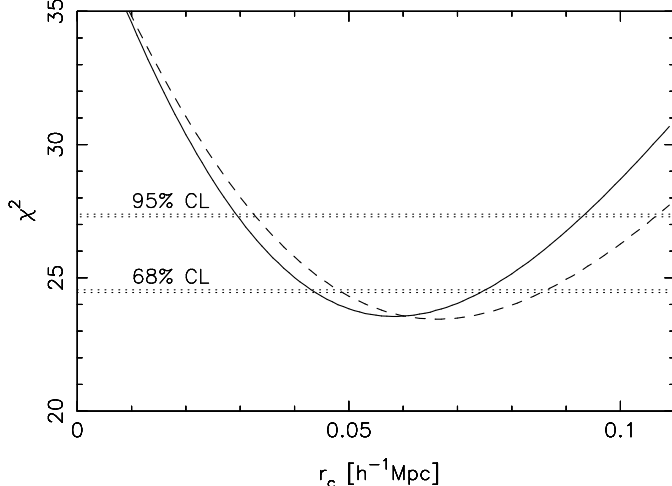


FIG. 3.— Constraints on the core radius  $r_c$  for a NSIS profile (solid line: SCDM; dashed line:  $\Lambda$ CDM).

As shown in Table 1, the inclusion of an additional SIS mass

profile did not significantly alter the best fit parameter values, and the quality of the fits was also not strongly affected. Not surprisingly, it is seen that with the inclusion of an extra mass component with a steep  $r^{-2}$  slope in the center, the best-fit inner slope of our generalized NFW model needs to become slightly shallower to match the observed shear. Figure 2 shows 2-parameter joint confidence regions for  $c_{\text{vir}}$  and  $\alpha$  for the  $\Lambda$ CDM cosmology. For the  $\alpha = 1$  case, the confidence intervals for  $c_{\text{vir}}$  are found to be consistent with the range of concentration parameters for  $M_{\text{vir}} = 2 \times 10^{15} h^{-1} M_{\odot}$  halos predicted from N-body simulations by Bullock et al. (2001).

TABLE 1  
BEST FIT MODEL PARAMETERS.

| Parameter        | SCDM ( $\Omega_m = 1, \Omega_\Lambda = 0$ )              |                |                       |                |
|------------------|--|----------------|-----------------------|----------------|
|                  | Generalized-NFW  |                | Generalized-NFW + SIS |                |
| $c_{\text{vir}}$ | Best fit value   | 68% conf. int. | Best fit value        | 68% conf. int. |
| $\alpha$         | 1.3  | 0.2–4.2        | 1.3                   | 0.3–2.8        |
| $r_{\text{vir}}$ | 1.5  | 0.9–1.6        | 1.4                   | 1.1–1.6        |
| $r_{\text{vir}}$ | 1.34   | 1.28–1.49      | 1.34                  | 1.28–1.43      |
| Parameter        | $\Lambda$ CDM ( $\Omega_m = 0.3, \Omega_\Lambda = 0.7$ ) |                |                       |                |
|                  | Generalized-NFW  |                | Generalized-NFW + SIS |                |
| $c_{\text{vir}}$ | Best fit value   | 68% conf. int. | Best fit value        | 68% conf. int. |
| $\alpha$         | 1.7  | 0.4–2.6        | 2.1                   | 0.2–4.8        |
| $r_{\text{vir}}$ | 1.4  | 1.3–1.6        | 1.3                   | 0.9–1.6        |
| $r_{\text{vir}}$ | 1.97   | 1.91–2.03      | 1.91                  | 1.79–2.10      |

We also fitted our data to a non-singular isothermal sphere (NSIS) model on the form  $\rho(r) = \sigma_v^2 / [2\pi G(r^2 + r_c^2)]$ , where  $r_c$  is the core radius. Our data were also well described by this model, with a best fit  $\chi^2/d.o.f. = 23.5/22$  for both SCDM and  $\Lambda$ CDM. Our best fit values were  $r_c = 58 h^{-1} \text{ kpc}$  and  $r_c = 66 h^{-1} \text{ kpc}$  for SCDM and  $\Lambda$ CDM, respectively. The best fit model curve is plotted in Figure 1, and the resulting 68% and 95% confidence intervals for  $r_c$  are shown in Figure 3.

## 5. DISCUSSION

We find that the average density profile of 6 massive clusters is well fitted by a generalized-NFW model with central slope  $\alpha \sim 0.9 - 1.6$ . This (steep) slope fits well with predictions from collisionless CDM simulations. The best fit slope of  $\alpha = 1.3 - 1.5$  is slightly steeper than the canonical NFW value, although  $\alpha = 1$  is only disfavored at less than 90% confidence for any of the models. For  $\Lambda$ CDM,  $\alpha \lesssim 0.5$  can be excluded with 95% confidence. The inclusion of an additional SIS mass profile corresponding to a massive central galaxy only resulted in minor changes for the best fit parameters. This indicates that any additional mass component associated with the central galaxy does not make a significant contribution to the total projected density on the scales that we probe in our weak lensing study.

Our constraints on  $\alpha$  are compatible with recent strong lensing studies of massive clusters: Smith et al. (2001) estimate  $\alpha = 1.3$  for A383 and Gavazzi et al. (2002) find  $0.7 \leq \alpha \leq 1.2$  for MS2137-23 (see, however, Sand, Treu & Ellis 2002, who find a best fit  $\alpha = 0.35$  and  $\alpha < 0.9$  at 99% CL for the same cluster). Our results are also consistent with recent X-ray cluster studies based on Chandra data: Arabadjis, Bautz, & Garmire (2002) find that the mass profile of CL 1358+6245 is well fit by a standard-NFW  $\alpha = 1$  profile, and Lewis, Buote, & Stocke (2003) find  $\alpha = 1.19 \pm 0.04$  for the central slope of A2029.

We find that an isothermal sphere model with a softened core can also produce a good fit to our data. This indicates that our weak lensing data is unable to discriminate between an outer slope of  $r^{-2}$  and  $r^{-3}$ . A pure SIS model is however strongly

excluded at the 99.9% CL (see Fig. 3). Yoshida et al. (2000) use simulations to study the effect of self-interacting dark matter on the structure of cluster halos. They find that even a small elastic collision cross-section of  $\sigma_* = 0.1\text{cm}^2\text{g}^{-1}$  will significantly affect the central density profile. Meneghetti et al. (2001) study the strong lensing properties of the cluster models of Yoshida et al. (2000), and find that even a cross-section as small as  $0.1\text{cm}^2\text{g}^{-1}$  is incompatible with the observed abundances of strongly lensed radial and tangential arcs in clusters. Their study is based on a simulated cluster at  $z = 0.278$  of final virial mass  $7.4 \times 10^{14}h^{-1}M_\odot$  in a  $\Lambda$ CDM universe. This cluster is at a similar redshift as the clusters in our data set, but our clusters are on average about twice as massive. From the  $r_c$  values tabulated by Meneghetti et al. (2001), we find that the predicted core radius for  $\sigma_* = 0.1\text{cm}^2\text{g}^{-1}$  of  $r_c = 80h^{-1}$  kpc is similar to our  $1\sigma$  (and  $2\sigma$ ) upper limit for the core radius shown in Figure 3. Here, we have taken into account a factor  $\sqrt{3}$  difference in the definition of  $r_c$  and a  $M^{1/3}$  scaling of lengths. A cross-section of  $1\text{cm}^2\text{g}^{-1}$  would produce a core radius of  $180h^{-1}$  kpc, which is strongly excluded by our data. In the small mean free path limit of “fluid” dark matter, a core-collapse producing a SIS-

type profile is expected. This is strongly excluded by our data, and the fluid limit is also excluded by the observed ellipticities of clusters (Miralda-Escudé 2002).

Davé et al. (2001) show that cross-sections of order  $5\text{cm}^2\text{g}^{-1}$  are needed to produce a good fit to the large apparent cores in dwarf galaxies. By introducing a velocity-dependent interaction cross-section for the dark matter particles, it may still be possible to reconcile our results with a self-interacting dark matter model that can produce constant-density cores in dwarf galaxies. Even if such a model may still be allowed, its velocity-dependence is already strongly confined by other astrophysical constraints, including the demographics of supermassive black holes in galaxy nuclei (Hennawi & Ostriker 2001).

It should be noted that even though dark matter models which produce large constant-density cores on clusters scales appear to be ruled out, many of the non-standard dark matter models are easily compatible with cusped cluster halos. One example is warm dark matter where the thermal velocity of the dark matter particles can erase the cusps of dwarf galaxy halos, but almost not affect more massive halos at all.

#### REFERENCES

- Arabadjis, J. S., Bautz, M. W., & Garmire, G. P. 2002, *ApJ*, 572, 66  
 Briel, U., & Henry, J. P. 1993, *A&A*, 278, 379  
 Broadhurst, T., Huang, X., Frye, B., & Ellis, R. 2000, *ApJ*, 534, L15  
 Bullock, J. S., Kolatt, T. S., Sigad, Y., Somerville, R. S., Kravtsov, A. V., Klypin, A. A., Primack, J. R., & Dekel, A. 2001, *MNRAS*, 321, 559  
 Cen, R. 2001, *ApJ*, 546, L77  
 Clowe, D., Luppino, G. A., Kaiser, N., & Gioia, I. M. 2000, *ApJ*, 539, 540  
 Clowe, D. & Schneider, P. 2001, *A&A*, 379, 384  
 Colín, P., Avila-Reese, V., & Valenzuela, O. 2000, *ApJ*, 542, 622  
 Czoske, O., Moore, B., Kneib, J.-P., & Soucail, G. 2002, *A&A*, 386, 31.  
 Dahle, H., Kaiser, N., Irgens, R. J., Lilje, P. B., & Maddox, S. J. 2002, *ApJS*, 139, 313  
 Dalcanton, J. J. & Bernstein, R. A. 2000, *ASP Conf. Ser.* 197, 161  
 Davé, R., Spergel, D. N., Steinhardt, P. J., & Wandelt, B. D. 2001, *ApJ*, 547, 574  
 de Blok, W. J. G., McGaugh, S. S., Bosma, A., & Rubin, V. C. 2001, *ApJ*, 552, L23  
 Gavazzi, R., Fort, B., Mellier, Y., Pelló, R. & Dantel-Fort, M. 2002, preprint (astro-ph/0212214)  
 Gelato, S. & Sommer-Larsen, J. 1999, *MNRAS*, 303, 321  
 Goodman, J. 2000, *New Astronomy*, 5, 103  
 Hannestad, S., & Scherrer, R.J. 2000, *Phys. Rev. D*, 62, 043522  
 Hennawi, J. F. & Ostriker, J. P. 2002, *ApJ*, 572, 41  
 Hoekstra, H., Franx, M., Kuijken, K., & van Dokkum, P. G. 2002, *MNRAS*, 333, 911  
 Hu, W., Barkana, R., & Gruzinov, A. 2000, *Phys. Rev. Lett.*, 85, 1158  
 Irgens, R. J., Lilje, P. B., Dahle, H., & Maddox, S. J. 2002, *ApJ*, 579, 227  
 Jing, Y. P. 2000, *ApJ*, 535, 30  
 Jing, Y. P. & Suto, Y. 2000, *ApJ*, 529, L69  
 Kaiser, N. & Squires, G. 1993, *ApJ*, 404, 441  
 Kaplinghat, M., Knox, L., & Turner, M. S. 2000, *Phys. Rev. Lett.*, 85, 3335  
 Keeton, C. R. & Madau, P. 2001, *ApJ*, 549, L25  
 Klypin, A., Kravtsov, A. V., Valenzuela, O., & Prada, F. 1999, *ApJ*, 522, 82  
 Lewis, A. D., Buote, D. A., & Stocke, J. T. 2003, *ApJ*, 586, 135  
 Meneghetti, M., Yoshida, N., Bartelmann, M., Moscardini, L., Springel, V., Tormen, G., & White, S. D. M. 2001, *MNRAS*, 325, 435  
 Miralda-Escudé, J. 2002, *ApJ*, 564, 60  
 Molikawa, K. & Hattori, M. 2001, *ApJ*, 559, 544  
 Moore, B., Quinn, T., Governato, F., Stadel, J., & Lake, G. 1999, *MNRAS*, 310, 1147  
 Moore, B., Ghigna, S., Governato, F., Lake, G., Quinn, T., Stadel, J., & Tozzi, P. 1999, *ApJ*, 524, L19  
 Navarro, J. F., Frenk, C. S., & White, S. D. M. 1996, *ApJ*, 462, 563  
 Navarro, J. F., Frenk, C. S., & White, S. D. M. 1997, *ApJ*, 490, 493  
 Navarro, J. F. & Steinmetz, M. 1997, *ApJ*, 478, 13  
 Navarro, J. F. & Steinmetz, M. 2000, *ApJ*, 538, 477  
 Oegerle, W. R. & Hoessel, J. G. 1991, *ApJ*, 375, 15  
 Oguri, M., Taruya, A., & Suto, Y. 2001, *ApJ*, 559, 572  
 Peebles, P. J. E. 2000, *ApJ*, 534, L127  
 Salucci, P. & Burkert, A. 2000, *ApJ*, 537, L9  
 Sand, D. J., Treu, T., & Ellis, R. S. 2002, *ApJ*, 574, L129  
 Shapiro, P. R. & Iliev, I. T. 2000, *ApJ*, 542, L1  
 Smith, G. P., Kneib, J., Ebeling, H., Czoske, O., & Smail, I. 2001, *ApJ*, 552, 493  
 Sommer-Larsen, J. & Dolgov, A. 2001, *ApJ*, 551, 608  
 Sommer-Larsen, J., Götz, M., & Portinari, L. 2002, *Ap&SS*, 281, 519  
 Spergel, D. N. & Steinhardt P. J. 2000, *Phys. Rev. Lett.*, 84, 3760  
 Tyson, J. A., Kochanski, G. P., & dell’Antonio, I. P. 1998, *ApJ*, 498, L107  
 Williams, L. L. R., Navarro, J. F., & Bartelmann, M. 1999, *ApJ*, 527, 535  
 Yoshida, N., Springel, V., White, S. D. M., & Tormen, G. 2000, *ApJ*, 544, L87  
 Zhao, H. 1996, *MNRAS*, 278, 488